The Egyptian Journal of Remote Sensing and Space Sciences (2015) 18, 107–118

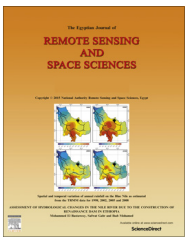
HOSTED BY

ELSEVIER

National Authority for Remote Sensing and Space Sciences

The Egyptian Journal of Remote Sensing and Space Sciences

www.elsevier.com/locate/ejrs
www.sciencedirect.com



RESEARCH PAPER

Assessing land-use changes driven by river dynamics in chronically flood affected Upper Brahmaputra plains, India, using RS-GIS techniques

Nabajit Hazarika, Apurba Kumar Das *, Suranjana Bhaswati Borah

School of Sciences, Department of Environmental Science, Tezpur University, Tezpur 784028, Assam, India

Received 8 August 2014; revised 23 January 2015; accepted 18 February 2015
Available online 19 March 2015

KEYWORDS

Land-use change;
River dynamics;
Hybrid classification;
Upper Brahmaputra

Abstract This work documents land-use changes driven by river dynamics along two tributaries in the chronically flood affected Upper Brahmaputra floodplain which supports a population of more than half a million. Planform changes for a period of 40 years are documented using topographical map and Landsat data, and the associated land-use change is assessed by utilising hybrid classification in GIS environment. Quantification of bankline migration shows that the river courses are unstable. A reversal in the rate of erosion and deposition is also observed. Hybrid classification of Landsat images yielded a higher level of accuracy as evident from the confusion matrixes. Overall, the accuracy of land-use classification ranged between 88.5% and 96.25%. Land-use change shows that there is an increase in settlement and agriculture and a decrease in the grassland. The area affected by erosion–deposition and river migration comprises primarily of the agricultural land. Effect of river dynamics on settlements is also evident. Loss of agricultural land and homestead led to the loss of livelihood and internal migration in the floodplains. The observed pattern of river dynamics and the consequent land-use change in the recent decades have thrown newer environmental challenges at a pace and magnitude way beyond the coping capabilities of the dwellers.

© 2015 National Authority for Remote Sensing and Space Sciences. Production and hosting by Elsevier B.V. This is an open access article under the CC BY-NC-ND license (http://creativecommons.org/licenses/by-nc-nd/4.0/).

1. Introduction

Floodplains are valuable ecosystems performing important functions and providing space for habitats and food production. Floodplains are considered to be one of the most endangered ecosystems worldwide as they are facing degradation by river regulations and enhanced land-use pressure. They are extensively cultivated all over the globe (Tockner et al., 2008; El Bastawesy et al., 2013; Qureshi et al., 2008) and serve as the primary source of income especially in South-East Asia. Floodplains are subjected to seasonal and periodical modifications as a result of lateral and vertical mobility of rivers driving a change in the land use pattern.

* Corresponding author. Tel.: +91 03712 275605, +91 9435490582; fax: +91 03712 267005.
E-mail address: apurba@tezu.ernet.in (A.K. Das).

Peer review under responsibility of National Authority for Remote Sensing and Space Sciences.

http://dx.doi.org/10.1016/j.ejrs.2015.02.001

1110-9823 © 2015 National Authority for Remote Sensing and Space Sciences. Production and hosting by Elsevier B.V.
This is an open access article under the CC BY-NC-ND license (http://creativecommons.org/licenses/by-nc-nd/4.0/).

Brahmaputra is the seventh largest river in the world (Hovius, 1998; Tandon and Sinha, 2007) and has created a thick extensive valley in the state of Assam, India. The valley supports about 27 million people by providing land for agriculture and human habitat. About 99% of total area of the State is rural. The net cultivated area of the State is 28.11 lakh hectares which is about 88% of the total land available for agricultural cultivation in the State (Economic Survey of Assam, 2011–12). More than 83% of the farmer families are small and marginal with an average operational holding as low as 1.15 hectare (Agricultural Census of Assam, 2005–06).

The Upper Brahmaputra plain is one of the worst flood-affected areas in India. Brahmaputra and its north bank tributaries regularly inundate and erode the floodplains damaging land and standing crops. As majority of the population depend upon cultivation for their lives and livelihood, land is of utmost importance. Changes in the land use and land cover (LULC) due to flooding, erosion and deposition are an obvious phenomenon in any floodplain, but these changes can be imperative to the people of Upper Brahmaputra due to overdependence on floodplain cultivation. Loss of land accounts for a significant loss in livelihood and may lead to displacement as most of the people here are marginal farmers. Socio-economic impoverishment and marginalisation is the fate of the displacees induced by river bank erosion (Haque, 1988; Hutton and Haque, 2003, 2004).

The dynamic nature of Brahmaputra and its tributaries modifies the floodplains frequently, at times to an undesired magnitude (Das et al., 2012; Goswami et al., 1999; Kotoky et al., 2004; Lahiri and Sinha, 2012; Sarma and Phukan, 2004). However, the associated changes in LULC (linking it with river dynamics) are rarely documented in quantitative terms (Kotoky et al., 2012; Mondal et al., 2013) which are essential preconditions for the formulation of floodplain management programme. LULC inventories are increasingly utilised in land-use planning, forest management and floodplain management (Bocco et al., 2001; Kotoky et al., 2012; Mahajan and Panwar, 2005; Schulz et al., 2010; Sun et al., 2009; Sylla et al., 2012; Boori et al., 2015).

Studies on LULC change are also important from the perspective of studying global environmental change and sustainable development highlighting the intensity and pattern of relationship between the human and earth (Jiyuan et al., 2010). Considering the importance of documenting LULC changes and the dearth of the same from a predominantly riverine region, the present work attempts to quantify changes in the land-use pattern in response to dynamics of two rivers Gai and Simen in Upper Brahmaputra plains. This study not only contributes to floodplain management but also throws light on the facets of riverine hazards that the people of this region face as a consequence of fluvial dynamics of the rivers.

Change detection of the land-use and land-cover requires accurate and timely data of different land-utilisation categories of an area (El Bastawesy et al., 2008, 2013a,b; Mohamed et al., 2014). In this regard remote sensing data facilitate the required information by providing timely and accurate data. In contrast to traditional ground-surveys, it provides a synoptic view of larger area over varied time span, hence providing more information regarding the land-use pattern in less time and in a cost-effective manner (Rogan and Chen, 2004; Yuan et al., 2005). Remotely sensed data coupled with GIS techniques have been effectively used by many workers to detect multi-temporal changes in LULC (Coppin et al., 2004; Kotoky et al., 2012; Mohamed and Verstraeten, 2012; Rogan and Chen, 2004; Rawat et al., 2013; Sun et al., 2009; Singh, 1989; Yuan et al., 2005). LULC changes in this work are documented using Landsat data with the help of hybrid classification, details of which are discussed in the methodology section.

2. Study area

This study concentrates in the Upper Brahmaputra floodplain drained by Gai and Simen – two dynamic North-bank tributaries of the River Brahmaputra, Assam, India (Fig. 1). These rivers originate in the Eastern Himalayas, carry heavy sediment loads, and enter the plains through narrow outlets with a great velocity. The study area is tectonically active (Lahiri and Sinha, 2012). The catchments, both in the mountain and plain, experience heavy rainfall during the monsoon season resulting in excess surface runoff inundating huge area in the plains used primarily for agricultural purposes. These rivers are flashy in nature and known to people of this region for bed aggradation.

The study area which lies between the latitude 27°15′0″N–27°57′16″N and longitude 94°12′18″E–95°30′0″E, is located in the Dhemaji district, with an elevation of about 100 m above the Mean Sea Level. It forms a narrow valley characterised by an abrupt drop in slope where the Himalayas merges into the plains and has a general gentle slope towards Brahmaputra. The climate of the region is Per-humid type characterised by high rainfall and a mild summer and winter. The area receives an annual rainfall of 2600–3200 mm (http://dhemaji.nic.in/climate.htm).

3. Data used and methods

Reconstructing historical channel movement by using historical maps and satellite images combined with GIS technique has been widely used (Das et al., 2012; Fuller et al., 2003; Harmar and Clifford, 2006; Kummu et al., 2008; Ollero, 2010; Sarma et al., 2007; Thakur et al., 2012; Winterbottom, 2000). This work adopts the regularly used approach of Remote Sensing and GIS techniques to delineate the river features for studying river dynamics and its impact on land-use in the neighbouring floodplains. The details of the dataset utilised in this study are presented in Table 1.

3.1. Image processing

The topographic maps used in this study are scanned and imported into Arc GIS format. The projections from the Landsat images are imported for georeferencing the topographical maps. Keeping a common projection minimises the error that occurs due to temporal changes. Landsat images for the dry season are utilised in order to avoid overestimation of the river expanse which is common with the images taken during high stages of flow. As part of radiometric corrections haze reduction, noise reduction and histogram equalisation are performed for all the satellite images in the ERDAS Imagine 11. Radiometric corrections are essential in change detection studies which consist of multi-date and multi-sensor satellite data. The corrections reduce inconsistencies in the satellite images which are inherent in the images because of differences

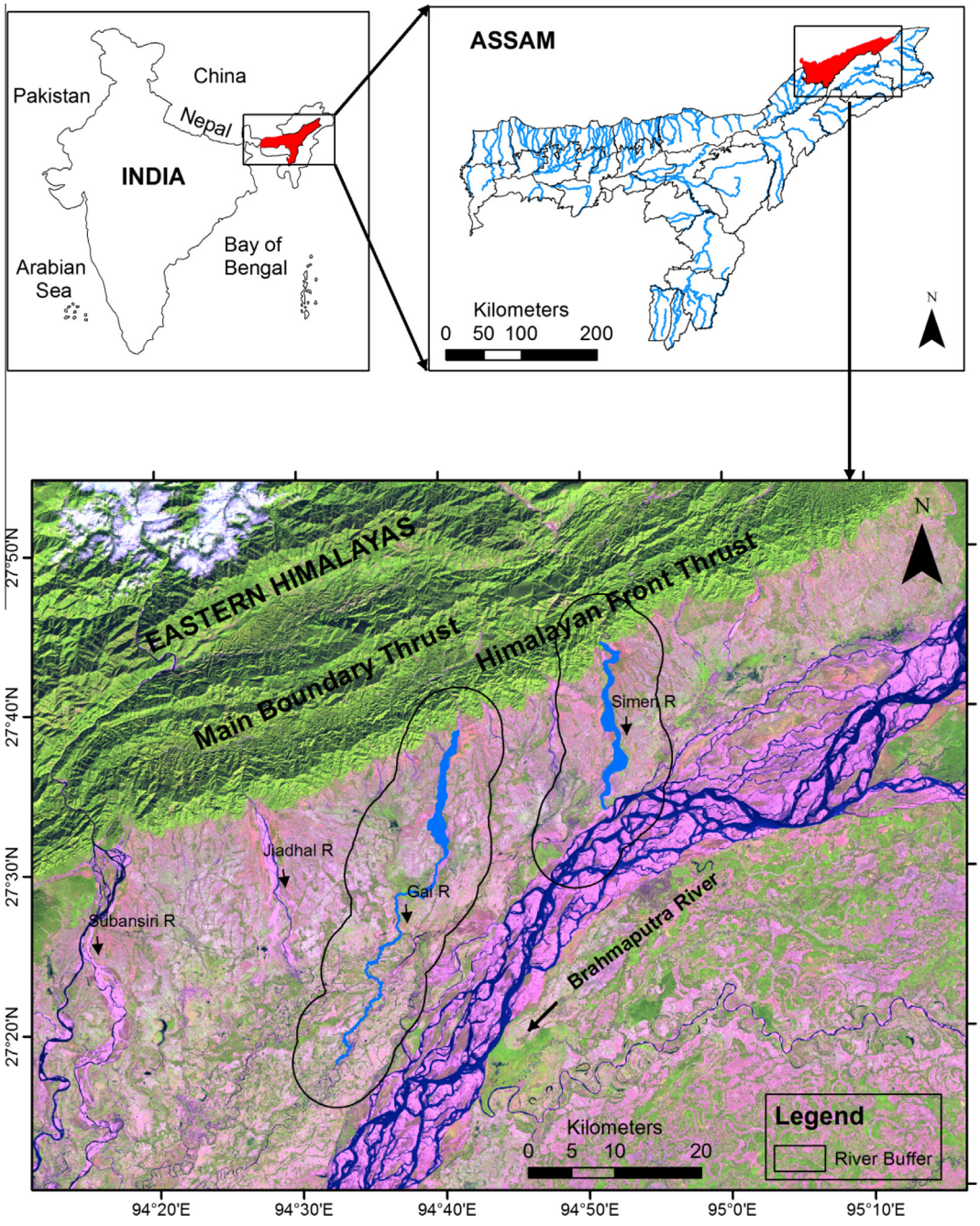


Figure 1 Location map of the study area with its physiographic setting and the studied stretch of the Gai and Simen rivers highlighted.

in acquisition conditions including variation in sun zenith angles (Chander et al., 2009; Mohamed and Verstraeten, 2012; Paolini et al., 2006; Yang and Lo, 2000). The banklines of the two rivers for the years 1970, 1990, 2000, and 2010 are delineated with the help of visual interpretation as well as digital image processing techniques. Contrast stretch, crisp, image filtering, different band combinations and image subtraction are utilised (Roy and Sinha, 2007). The delineated banklines are used to generate a channel centreline (the line connecting the central point intermediates between the two channel boundaries) with the help of onscreen digitisation (Nicoll and Hickin, 2010) in the Arc Map.

3.2. Planform parameters and change detection

For convenience of analysis the river channels are divided into 10 segments (A-J) with the help of equidistant sections calculated by an automated process in Arc GIS. Bankline migration, sinuosity, erosion, and deposition are measured and studied along these segments. The entire dataset is integrated into GIS environment to quantify the planform dynamics.

Sinuosity (S) is defined as the "total length of a reach (L) divided by the length of straight line (l) between the two points", $S = L/l$ (Stolum, 1996). The digitised centreline is divided into segments at each intersection of the valley axis.

Table 1 Dataset utilised in the study.

Data	Path/row	Resolution/scale	Year	Source
Landsat MSS	145/41	60 m	1973	Landsat.org
Landsat TM	135/41	30 m	1990	USGS[a]
Landsat ETM +	135/41	30 m	2000	USGS
Landsat TM	135/41	30 m	2010	USGS
Topographical Map		1:50000	1969–1970	SOI[b]

[a] USGS: United States Geological Survey.
[b] SOI: Survey of India.

And then the length of the centreline is divided by the length of the straight line between the two points.

Bankline migration is recorded for different periods using overlay analysis in GIS environment. The highest lateral shifts of the banks between different periods for each segment are recorded. The migration of the river banks for this study is considered to be of 'positive' (+) nature if it has the potential to bring large scale surface modifications in the floodplain and translate itself into fluvial hazard. Migration due to avulsion, progressive shifting of meander bends (unidirectional) and channel widening (where the banks moved away from each other) are considered as a positive change. When both the banks moved towards each other causing channel narrowing, it is considered as a negative (−) change as it does not hold any significant potential to cause changes in the floodplain.

For quantification of erosion and deposition the vectorised banklines are overlaid for different periods. The intersecting banks are vectorised as polygons for erosion (where the river migrated into a new position relative to the older channel) and deposition (polygons for previous position of the river) in each segment. Average rate of erosion and deposition is determined by dividing total erosion/deposition by the number of years elapsed between two successive observations (Goswami et al., 1999; Yao et al., 2011).

3.3. Land-use classification and assessment of effect of river dynamics

The floodplains adjacent to Gai and Simen rivers (within 5 km buffer, which is the highest extent of recorded river dynamics during study period) are classified into eight classes: river/waterbodies, wetland, settlement, agriculture, grassland, plantation, sand and forest using the ERDAS Imagine 11. These eight classes are representatives of the actual landscape in the study region and could be determined using a moderate resolution Landsat image. Hybrid classification, which involves the combination of both unsupervised and supervised classifications, for better representation of classes, is performed on the satellite images for different time periods (1973–2000). Unsupervised classification is initially executed on the images and the signatures obtained are clustered into meaningful classes of interest. A classification scheme is formulated for the process of classification which is shown in Table 2. These clustered signatures are used to reclassify the images using a maximum likelihood classifier which classifies the pixels based on the maximum probability of belonging to a particular class (Richards and Jia, 2006). The final classified images are then filtered using a neighbourhood majority function which replaces the centre pixel in the matrix with the most common data file value in the window for removal of noise and smoothening of classes. A 3×3 matrix is used for this purpose. Recoding is performed for major misclassification of features such as shadow. The accuracy of each classified image is assessed by a set of 400 random points for Gai and 300 for Simen based on the number of classes (50 points per class). These random points known as reference points are overlaid on the images and each point is assigned to one of the land-use classes. Topographical maps, careful examination of satellite image, high resolution Google Earth images for different periods, limited ground truthing and local knowledge about the area and changes over time are used for assigning classes.

Table 2 Classification scheme used for this study.

No.	Class	Description
1	River/ waterbodies	Open water features such as rivers, streams, lakes and reservoirs
2	Sand	Sandbars and other sand deposition areas including both dry and wet sand areas
3	Wetland	Low lying areas saturated with moisture and covered with aquatic vegetation such as water hyacinth
4	Grassland	Areas dominated by grasses including vegetated sandbars and grazing areas
5	Agriculture	Areas under cultivation including current fallow areas
6	Settlement	Areas under urban and rural built-up including homestead area
7	Plantation	Forest and agricultural plantations like orchards and tea gardens with significant patterns
8	Forest	Areas under dense and open forest and scrublands

For each map, a confusion matrix is created with each row representing land-use classes in the classified map and each column representing the reference land-use classes. From this matrix, overall accuracy and kappa co-efficient are calculated for each classified map. Kappa Co-efficient is a degree of agreement or correctness among the classified map and the reference data (Congalton, 1991; Rosenfield and Fitzpatrick, 1986). User's accuracy and producer's accuracy are also calculated. User's accuracy measures the proportion of each class which is correctly classified in the map as a particular class and producer's accuracy measures the proportion of land-use class which is correctly classified as the actual landscape

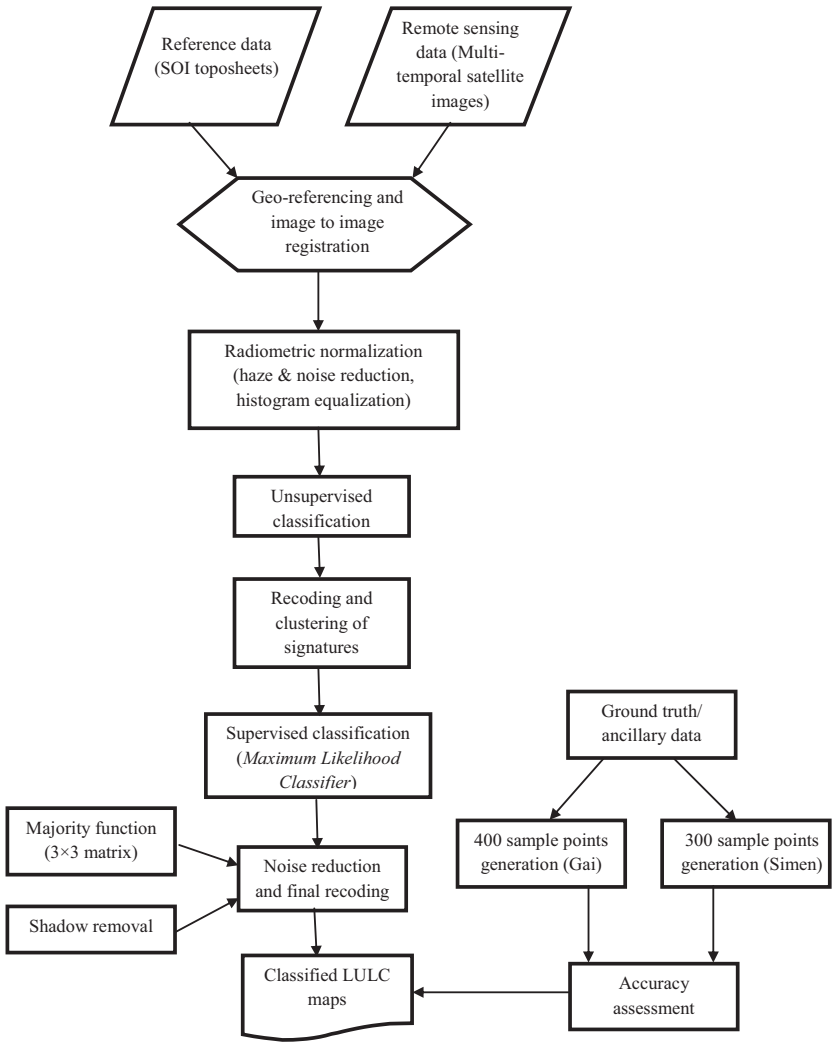


Figure 2 Schematic representation of the image processing and classification techniques.

present on the ground. The scheme of classification techniques employed for this study is shown in Fig. 2.

The erosion and deposition polygons for both the rivers are overlaid on the classified maps to extract the areas which are affected by these processes. Values are expressed in total area affected for each land-use category.

4. Results and discussion

4.1. Classification accuracy

The classified images (Fig. 3) show overall accuracies of 88.5, 91.25 and 96.25% for the Gai River in 1973, 1990 and 2000 with kappa co-efficients of 0.87, 0.9 and 0.95, respectively. For Simen, the overall accuracies are 92%, 94.33% and 92% in 1973, 1990 and 2000 with kappa co-efficients of 0.9, 0.93 and 0.9, respectively (Table 3) (the detailed confusion matrices for each classified image with their accuracies are shown in the Tables 4a–c for the Gai River and Tables 4d–e for the Simen River in the supplementary material). In all the classified images, forest is the best classified class with almost 100% accuracy because of its distinct separation from other classes. Water and sand pixels also show highly reliable accuracy except in some occasions where wet sand areas are confused between water and grassland. Grassland and settlement areas are usually confused with agricultural areas because of mixed pixels in transition areas. Most of the wetland areas are covered with water hyacinth and are occasionally confused with grassland areas. The overall classification accuracies suggest that the classification is reliable and acceptable for further analysis.

4.2. Bankline shift and changes in the sinuosity

Bankline shift in the Gai River is not uniform during the study. The mean shift in the left bank for the period 1970–1990 was 1.041 km, whereas a shift of about 1.39 km is recorded for the right bank during the same period. However, the mean shift in the left bank and the right bank for the period 2000–2010 is 0.692 km and 0.682 km, respectively. The stretches showing the highest mobility are located in the upstream of the river reach. The upper reaches of the Gai River between segments C and E showed the highest mobility. As a result of repetitive avulsion near its intersection with road/railways

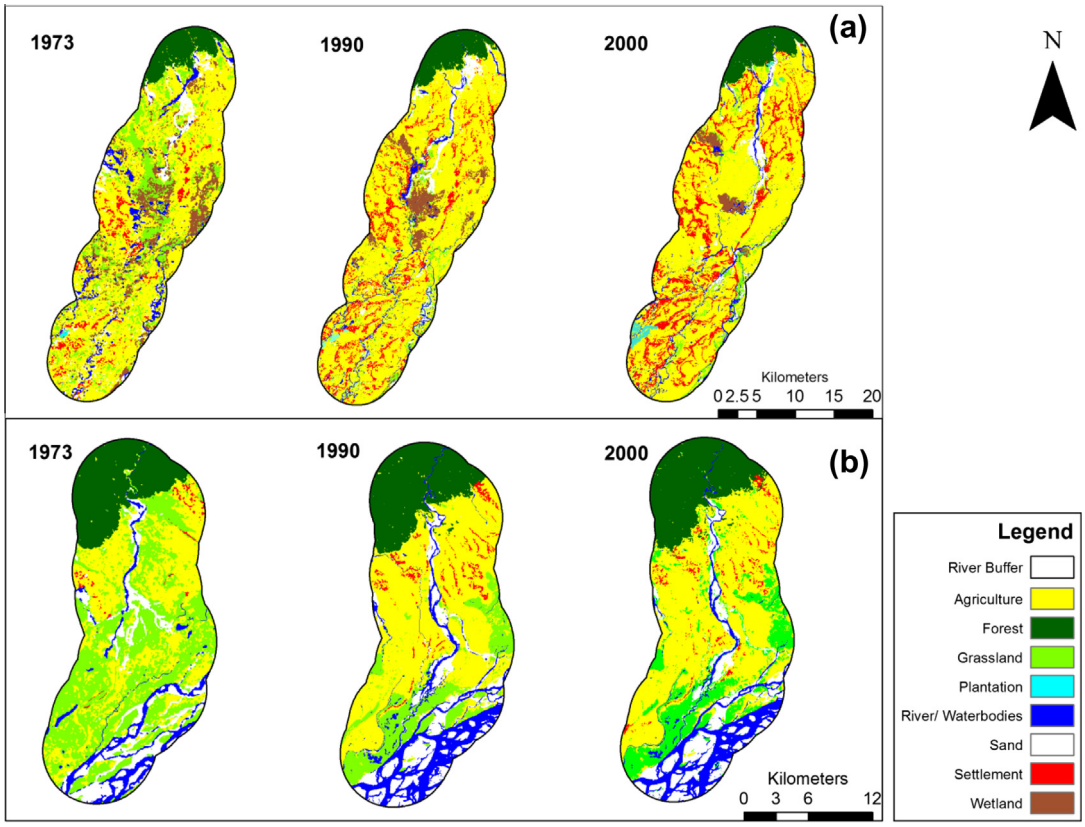


Figure 3 Land-use classes in different time periods along (a) The Gai River and (b) The Simen River in the Upper Brahmaputra plains, classified using hybrid classification scheme.

Table 3 Classification accuracy of the hybrid classification and K-statistics.

Accuracy	The Gai River			The Simen River		
	1973	1990	2000	1973	1990	2000
Overall Classification Accuracy (%)	88.50	91.25	96.25	92	94.33	92
Kappa Statistics (K)	0.8686	0.9	0.9571	0.904	0.932	0.904

the river migrated freely during the study period. Both the banks migrated ~5 km towards east in 1990–2000 (Fig. 4), which is the highest, recorded during the study period.

In comparison to the upper, lower reaches of the river Gai show slow and continuous migration of its banks by progressive shifting of its meander bends. Bend morphology of freely meandering river is an important indicator of its response towards changes in discharge and flow. Progressive shifting of meander bends is an intrinsic property of a meandering alluvial river by virtue of which it tends to maintain equilibrium in energy distribution (Leopold and Wolman, 1960). The Gai River develops discrete meander bends towards its lower reach. Several cases of neck and chute cutoff could be observed throughout the study period (Fig. 5a–c). Neck cutoff is a flood plain feature of a meandering river where the entire meander loop is abandoned (Lewis and Lewin, 1983). In monsoon season during high stages of flow the river meanders are breached by chute channels in different river reaches that connect the two closest bends of a meander. This causes the flow to abandon the meander and follow a straighter course downslope. It is rather a slow process and develops over a period of several years but floods may trigger it to occur suddenly. The sinuosity for the Gai River is shown in Fig. 6. The average sinuosity of the river shows a decreasing trend from 1.61 in 1970 to 1.37 in 2010. The decrease in sinuosity due to meander cutoffs has resulted in river shortening as evident from the reduced river length from 133.6 km to 111.74 km. The river is showing a transition from meandering to straight during the study period. Schumm (1963) attributed river straightening to increase in the bed material load as well as coarser sediments. Increasing trend of deposition in the river reaches during the recent decades is evident.

The overall direction of migration in the Gai River during the study period remained westward. This unidirectional-avulsive shift could be attributed to cross-valley tilting (Lahiri and Sinha, 2012).

As indicated by sinuosity, the course of the Simen River, compared to Gai, has been a straighter one in different periods

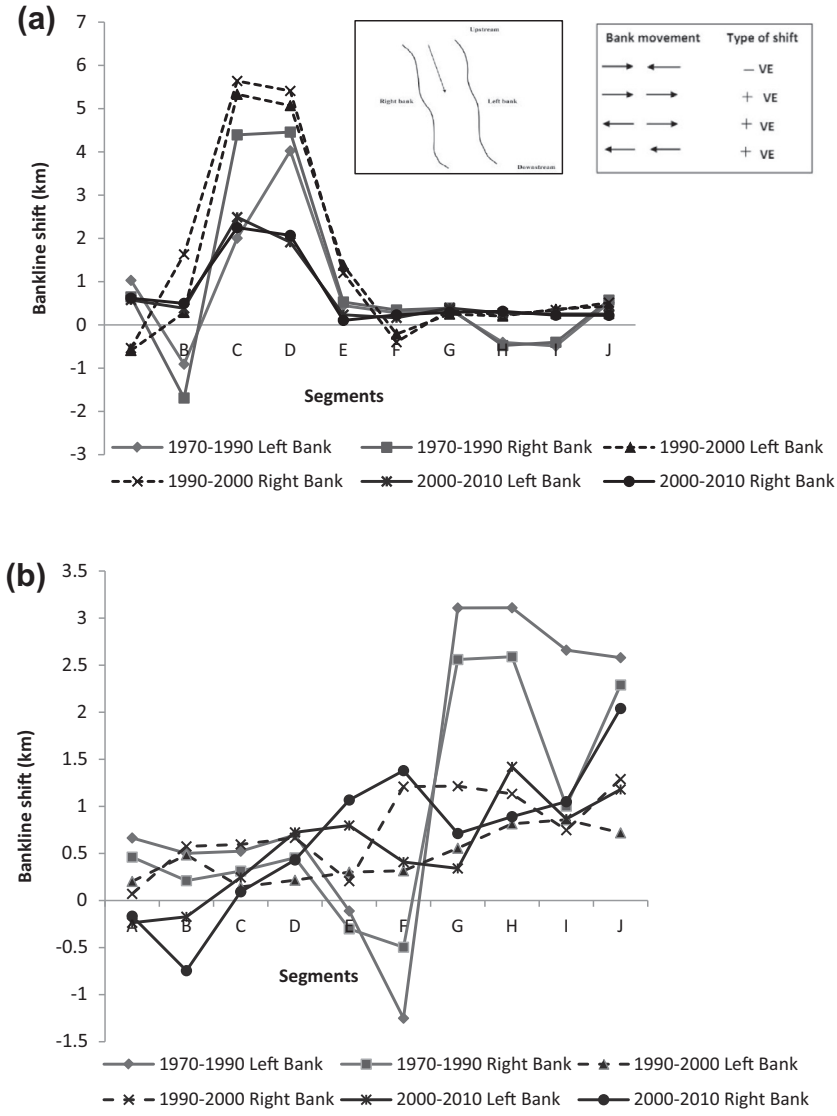


Figure 4 Bankline migration in the Gai River (a) and in the Simen River (b) during 1970–2010 in Upper Brahmaputra plains.

(Fig. 6). The upstream of the river shows a minimum mobility in most of the segments (Fig. 4). The mean movement for the left bank varied from 1.52 km during 1970–1990 to 0.64 km in 2000–2010. The right bank also showed a similar pattern of mobility with the mean movement ranging from 1.06 km (1970–1990) to 0.86 km (2000–2010). The process of meander cutoff is not very prominent in the Simen River but it underwent a significant shortening in length primarily due to migration of its confluence point (Fig. 5d). Channel confluences and their dynamics are significant to the river systems as they influence the morphology and hydrology of the upstream and downstream of the confluence. It affects the distribution of water in different reaches and sediment dispersal around the confluence point (Roy and Sinha, 2007).

The River Simen during 1970s travelled a length of 68.5 km before falling into the Brahmaputra but in 2010 the length is reduced to 45.96 km. Downstream reaches migrated continuously eastward during the study period, changing its confluence point and reaching Brahmaputra more rapidly. Periodic avulsion triggered by breaches in the embankment during high stages of flow caused such large scale movement of its banks changing the confluence point during the study period. During the period of 1970–1990 a very high degree of channel migration was recorded in the lower reaches (Fig. 5d). Between 1990 and 2000 the upper reaches of the river migrated eastward. The last segment continued its eastward migration changing the confluence of the river and joining the Brahmaputra River about 1.4 km eastward in comparison to its confluence point in the year 1990. The confluence further shifted eastward during 2000–2010 and in turn shortened the river course. In segments B, D and H the river migrated westward marginally but the overall direction of migration remains eastward.

4.3. Quantification of erosion and deposition

During 1970–1990 the upstream of Gai (segment A and B) shows high amount of erosion (Fig. 7). Overall, the river eroded an area of 719.42 ha at an annual rate of 35.97 ha/yr. Net loss of land during this period stands at 389.9 ha.

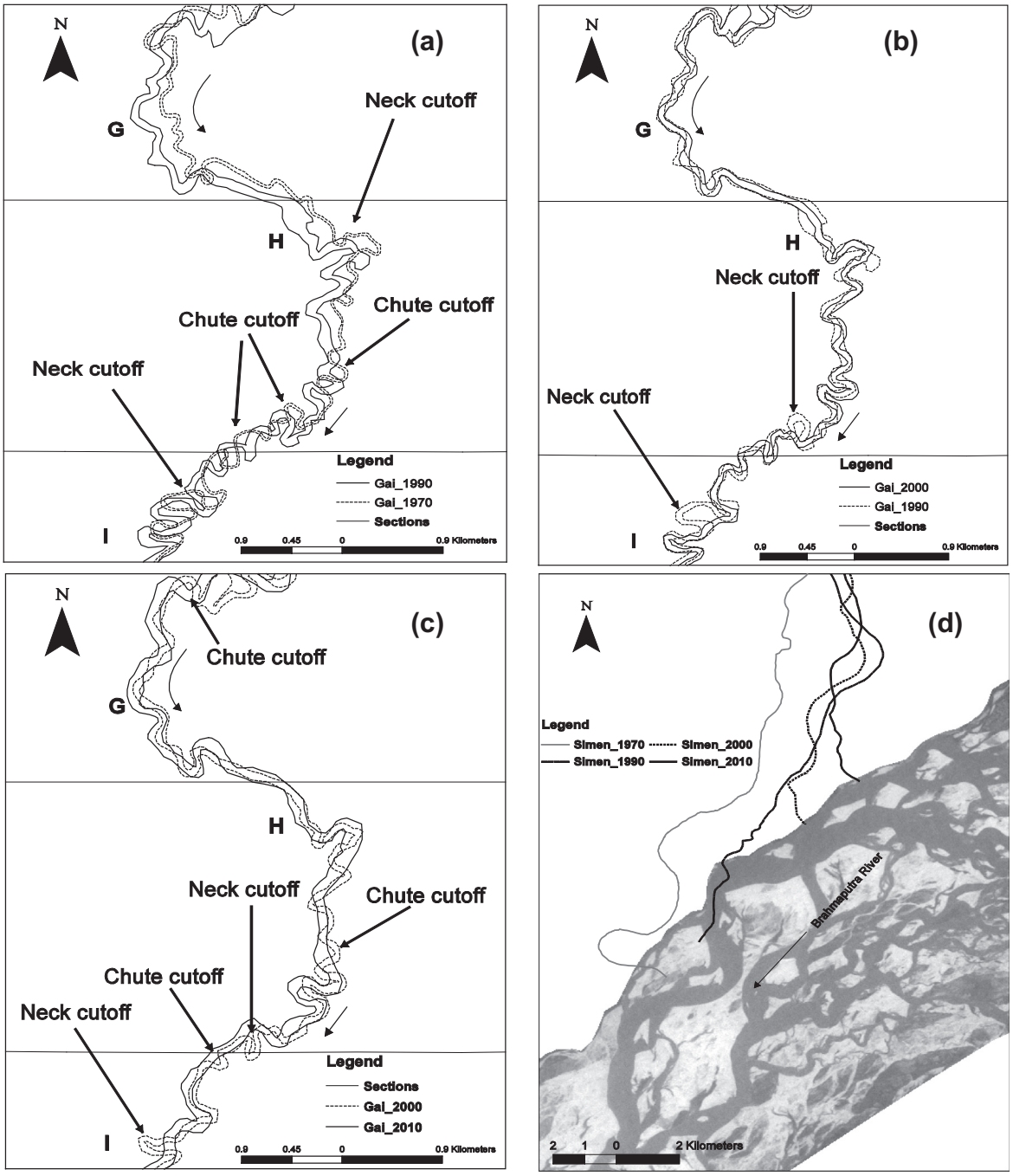


Figure 5 Process of meander cut-off in the Gai River during 1970–1990 (a), 1990–2000 (b), 2000–2010 (c), and confluence migration in the Simen River during 1970–2010 (d) in Upper Brahmaputra plains.

In 1990–2000, the rate of erosion is the highest; upstream having the highest share. Segments A and B incur a loss of 296.3 ha of fertile land which accounts for 68.64% of the overall erosion during the decade. This could be attributed to the high velocity of the river with which it enters the plains from the hills of the Eastern Himalayas which results in intense scouring in the upper reaches of the river. The overall erosion stands at 431.62 ha of land at an annual rate of 43.16 ha/yr. The net loss is found to be 70.44 ha.

In the most recent decade (2000–2010) the rate of erosion declined compared to the previous period. In the upper reaches of the river (segment A and B) where there was a dominance of erosion in the earlier periods, the deposition exceeded erosion in this decade. The river deposited sediments over an area of 171.88 ha between segment A and B, whereas, an area of 149.49 ha is eroded. This implies that an area of 22.39 ha of land is gained during this period in the upper reaches. In the context of cultivation this net area gain, however, is not beneficial because a major amount of area contains deposition of coarser sediments which makes the land unfertile. The total area eroded during this period is 334.04 ha at an annual rate of 33.4 ha/yr.

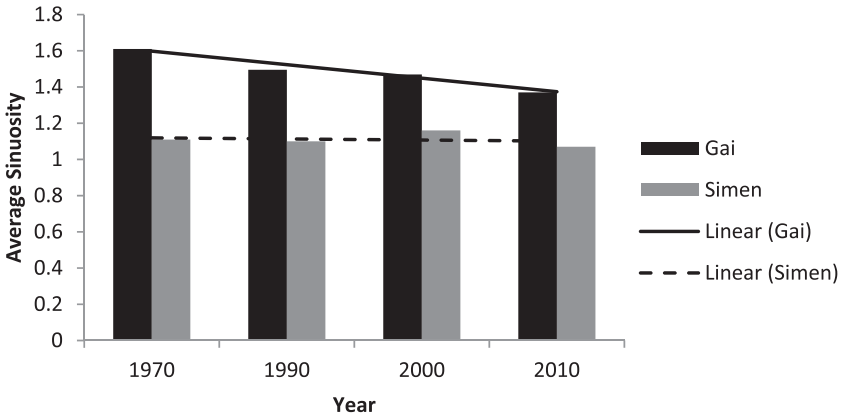


Figure 6 Trend of sinuosity for Gai and Simen rivers in upper Brahmaputra plains during 1970–2010.

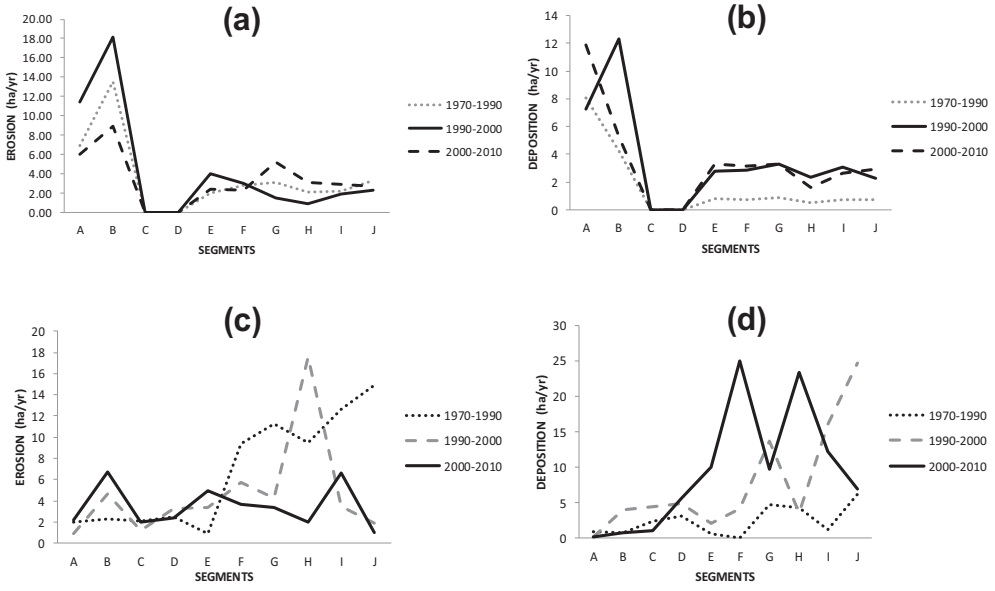


Figure 7 Account of erosion (a) and deposition (b) throughout the studied segments of the River Gai and in Simen (c) and (d) during 1970–2010 in Upper Brahmaputra plains.

The upstream of the River Gai during the entire study period has been dynamic in terms of erosion and deposition. The first 30 years show a dominance of erosion due to a high amount of scouring whereas the latter part is dominated by deposition which can be attributed to the river stabilisation in the form of embankments. In the last four decades total erosion by the Gai River is found to be 1485.08 ha at an annual rate of 37.14 ha/yr, while total deposition is 1031.59 ha at an annual rate of 25.8 ha/yr.

In the Simen River, during 1970–1990 erosion dominated the erosional–depositional process. The downstream of the river shows higher erosional rates than the upstream reaches (Fig. 7). Between Segments F to J the total erosion stands at ~1153 ha of fertile land which is 85.42% of the total erosion during the period of 20 years. This is resulted due to the concave bank erosion by the river in the downstream reaches and the process of confluence migration which dominated the river processes during the entire study period. The river overall eroded a land area of 1349.75 ha at an annual rate of 67.49 ha/yr.

In the latter two decades the erosional rates decreased and the rate of deposition increased. The amount of deposition (774.26 ha) exceeded the amount of erosion (461.40 ha) during 1990–2000. The only segment that shows a high rate of erosion (17.55 ha/yr) is downstream segment H. This is due to avulsions and the river shortening process by confluence migration that moved the confluence to further upstream and towards east in consecutive periods. In the last decade (2000–2010) the rate of deposition increased manifold (94.76 ha/yr). The total area eroded by the river during this period stands at 348.15 ha at an annual rate of 34.81 ha/yr.

The observed bankline shift, avulsion and confluence migration all indicate that these two rivers have been dynamic and actively changing the floodplain features. For both the rivers, the trend analyses of erosional and depositional patterns (Fig. 8) clearly suggest an increase in the rates of deposition compared to the rate of erosion in the recent time.

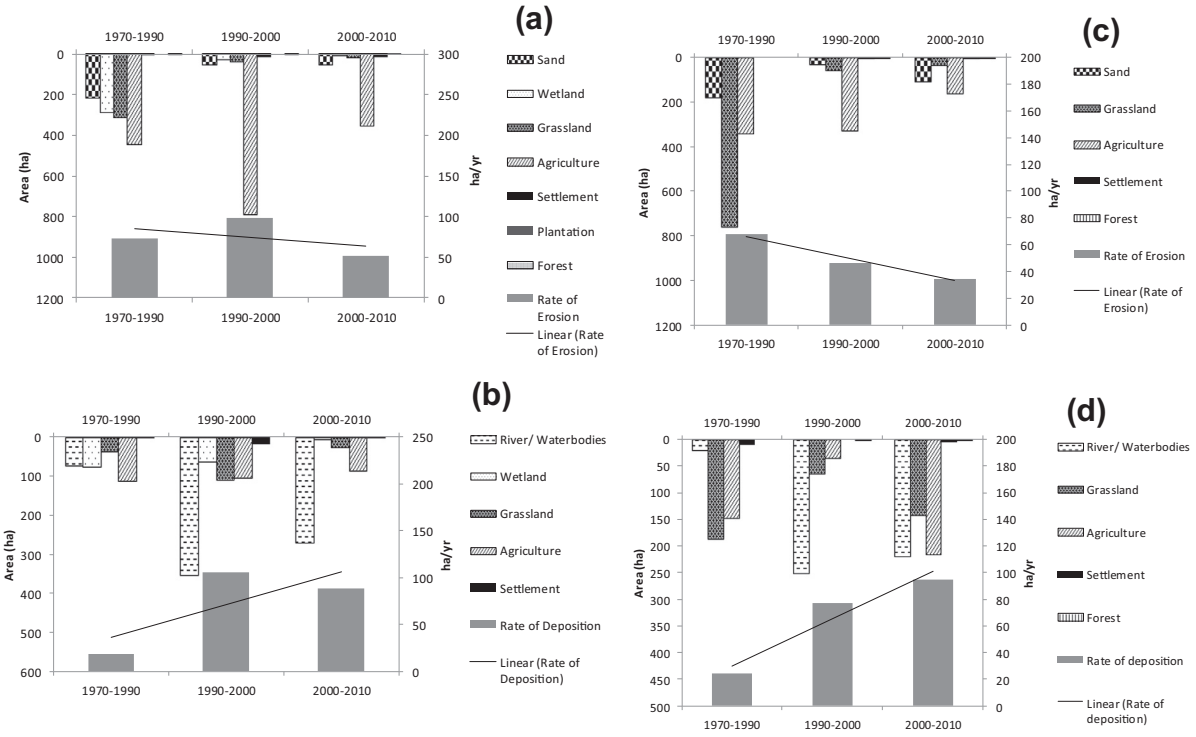


Figure 8 Land-use classes affected due to erosion (a) and deposition (b) by the Gai River and by the Simen River (c) and (d) with trends of erosion–deposition during 1970–2010 in Upper Brahmaputra plains. Note the reversal of process dominance in terms of erosion and deposition in both the rivers in recent time.

4.4. Effect of river dynamics on land-use

In case of the Gai River, it is observed that the highly affected areas by erosion throughout the years are agricultural land followed by grassland and wetland. Agriculture comprised of about 31%, 80% and 69% of the total eroded area in 1970–1990, 1990–2000 and 2000–2010, respectively. Average annual rates of erosion from 1970 to 2010 show a decreasing trend. In case of deposition, it is most discernible in the land-use class river/waterbodies, suggesting migration of the active channel. Higher deposition is also observed in agricultural areas followed by grassland and wetland areas. The trend of deposition shows a gradual increase from 1970 to 2010. The areas affected by erosion and deposition in the chosen time periods with their annual rates and trend are depicted in Fig. 8.

In River Simen, agriculture consists of 25%, 71% and 47% of the total eroded areas in 1970–1990, 1990–2000 and 2000–2010, respectively. This temporal pattern of area affected by erosion is similar to that of the Gai River. It may be noted that grassland was the dominant land-use class in 1970–1990. It comprised of 56% of the total landscape. In later years this percentage share decreased noticeably. Classification statistics for entire 5 km buffer areas around the Gai and Simen rivers show an increase in agricultural and settlement areas and decrease in grassland and wetland areas over the years. The increased influence of erosion on agricultural land in the recent decades could be attributed to this conversion of grassland into agricultural land. These two land-use classes are also equally affected by deposition (Fig. 8).

In the overall context of this work, another land-use class that merits a discussion is the settlement. Erosion and deposition by both the rivers affected settlement areas in the floodplains. The Gai River eroded 7.8, 19.57 and 17.78 hectares of land under settlement class during 1970–1990, 1990–2000 and 2000–2010, respectively. Deposition by the Gai River leads to casting of sand over an area of 1.3, 17.06 and 2.52 hectares in 1970–1990, 1990–2000 and 2000–2010 respectively under settlement. Similarly, the Simen River eroded an area of 10.88 and 10.39 hectares of land during 1990–2000 and 2000–2010, respectively and deposited sediments over an area of 12.02 and 6.58 hectares during 1970–1990 and 2000–2010 respectively under settlement. Though the figures are small in terms of area, but in terms of socio-economic stress the impact is significant as it leads to loss of homestead. Loss of homestead coupled with livelihood leads to internal migration in the floodplains which is evident during field visits.

It may be mentioned here that similar to agriculture the settlement land-use class also shows an overall increase from 1970 to 2010 indicating a population growth in the floodplains (Fig. 3).

As LULC changes are forced by fluvial hazard, floodplain dwellers as an adjustment would further modify the land-use pattern which may lead to changes in the sediment flux in the longer run and again affect the river planform. This moulding and remoulding of land-use jeopardise the flood management policies and throw new challenges to the floodplain dwellers, at times way beyond their capacity to cope up.

5. Conclusions

In this study river dynamics along with land-use in an active floodplain of a large tropical river is analysed. The analyses reflect that more and more of the floodplains are being put to human activities, especially agriculture. As mentioned

earlier that the river morphology and land-use is intricately related, the increased human interventions are a potential agent of altering an already endangered ecosystem. This increase in floodplain usage for human activities is expected to continue in near future with the given trend of high population growth in the study region.

The result shows that most affected land-use class is agriculture. In the regional context this pattern of impact of river dynamics on land-use is of major concern as it directly influences livelihood of the floodplain dwellers. Analyses of river dynamics show frequent and large scale changes experienced in the floodplains of the study region. It is mentioned earlier that floodplains are the major component of the human habitat in this region; the active nature of the rivers and its impact on land-use, particularly on agriculture, reflect the newer environmental challenges that the dwellers of Brahmaputra floodplains are constantly faced with. In the current scenario of climate change the vulnerability of the floodplain dwellers towards environmental threats increases further.

Land-use for different periods was mapped using hybrid classification. This work shows that hybrid classification using Landsat images is an effective tool in studies aimed at land-use analysis. Change in land-use pattern in association with river dynamics can be effectively used as an indicator of evaluating socio-economic impact of riverine hazards on human beings. If it is performed with a higher resolution data these indicators could be utilised to assess socio-economic impact at micro scales.

Acknowledgements

The first author is a recipient of UGC fellowship and UGC is acknowledged for the same. SBB is recipient of DST fellowship and hence acknowledges DST. USGS, SOI and Landsat.org are acknowledged for their data.

Appendix A. Supplementary data

Supplementary data associated with this article can be found, in the online version, at http://dx.doi.org/10.1016/j.ejrs.2015.02.001.

References

Agricultural Census of Assam, 2005–06. Directorate of Economics and Statistics, Govt. of Assam, India. <http://ecostatassam.nic.in/agri_%20agri%20census%20report%202005-06.pdf> (retrieved on 14.07.2014).

Bocco, G., Mendoza, M., Velazquez, A., 2001. Remote sensing and GIS-based regional geomorphological mapping- a tool for land use planning in developing countries. Geomorphology 39, 211–219.

Boori, M.S., Vozenilek, V., Choudhary, K., 2015. Land use/cover disturbance due to tourism in Jeseniky Mountain, Czech Republic: a remote sensing and GIS based approach. Egypt. J. Remote Sens. Space Sci. 18 (1), 17–26.

Chander, G., Markham, B.L., Helder, D.L., 2009. Summary of current radiometric calibration coefficients for Landsat MSS, TM, ETM+ and EO-1 ALI sensors. Remote Sens. Environ. 113 (5), 893–903.

Congalton, R.G., 1991. A review of assessing the accuracy of classifications of remotely sensed data. Remote Sens. Environ. 37, 35–46.

Coppin, P., Jonckheere, I., Nackaerts, K., Muys, B., Lambin, E., 2004. Digital change detection methods in ecosystem monitoring: a review. Int. J. Remote Sens. 25 (9), 1565–1596.

Das, A.K., Sah, R.K., Hazarika, N., 2012. Bankline change and the facets of riverine hazards in the floodplain of Subansiri-Ranganadi Doab, Brahmaputra Valley, India. Nat. Hazards 64, 1015–1028.

Economic Survey of Assam, 2011–12. Directorate of Economics and Statistics, Govt. of Assam, India. <http://www.ecostatassam.nic.in/ads_economic%20survey_2011-12.pdf> (retrieved on 14.07.2014).

El Bastawesy, M., Khalaf, F., Arafat, F., 2008. The use of remote sensing and GIS for the estimation of water loss from Tushka lakes, South Western Desert. Egypt. J. Afr. Earth Sci. 52, 73–80.

El Bastawesy, M., Gabr, S., White, K.H., 2013a. Hydrology and geomorphology of the Upper White Nile lakes and their relevance for water resource management in the Nile basin. Hydrol. Process. 27, 196–207.

El Bastawesy, M., Ramadan, A.R., Faid, A., El Osta, M., 2013b. Assessment of waterlogging in agricultural megaprojects in the closed drainage basins of the Western Desert of Egypt. Hydrol. Earth Syst. Sci. 17, 1493–1501.

Fuller, I.C., Large, A.R.G., Milan, D.J., 2003. Quantifying channel development and sediment transfer following chute cutoff in a wandering gravel-bed river. Geomorphology 54, 307–323.

Goswami, U., Sarma, J.N., Patgiri, A.D., 1999. River channel changes of the Subansiri in Assam, India. Geomorphology 30, 227–244.

Haque, C.E., 1988. Human adjustments to river bank erosion hazard in the Jamuna floodplain, Bangladesh. Human Ecol. 16 (4), 421–437.

Harmar, O.P., Clifford, N.J., 2006. Planform dynamics of the Lower Mississippi River. Earth. Surf. Processes Landforms 31, 825–843.

Hovius, N., 1998. Controls on sediment supply by larger rivers. In: Shanley, K.W., McCabe, P.J. (Eds.), Relative Role of Eustasy, Climate, and Tectonism in Continental Rocks. Society for Sedimentary Geology (SEPM), pp. 3–16, Special Publication, 59.

Hutton, D., Haque, C.E., 2003. Patterns of coping and adaptation among erosion-induced displacees in Bangladesh: implications for hazard analysis and mitigation. Nat. Hazards 29, 405–421.

Hutton, D., Haque, C.E., 2004. Human vulnerability, dislocation and resettlement: adaptation process of river-bank erosion-induced displacees in Bangladesh. Disasters 28 (1), 41–62.

Jiyuan, L., Zengxiang, Z., Xinliang, X., Wenhui, K., Wancun, Z., Shuwen, Z., Rendong, L., Changzhen, Y., Dongsheng, Y., Shixin, W., Nan, J., 2010. Spatial patterns and driving forces of land use change in China during the early 21st century. J. Geog. Sci. 20 (4), 483–494.

Kotoky, P., Bezbaruah, D., Baruah, J., Sarma, J.N., 2004. Nature of bank erosion along the Brahmaputra river channel, Assam, India. Curr. Sci. 88 (4), 634–640.

Kotoky, P., Dutta, M.K., Borah, G.C., 2012. Changes in landuse and landcover along the Dhansiri River Channel, Assam – a remote sensing and GIS approach. J. Geol. Soc. India 79, 61–68.

Kummu, M., Lu, X.X., Rasphone, A., Sarkkula, J., Koponen, J., 2008. Riverbank changes along the Mekong River: remote sensing detection in the Vientiane–Nong Khai area. Quat. Int. 186, 100–112.

Lahiri, S.K., Sinha, R., 2012. Tectonic controls on the morphodynamics of the Brahmaputra River system in the upper Assam valley, India. Geomorphology 169, 74–85.

Leopold, L.B., Wolman, M.G., 1960. River meanders. Geol. Soc. Am. Bull. 71, 769–793.

Lewis, G.W., Lewin, J., 1983. Alluvial cutoffs in Wales and the Borderlands. International Association of Sedimentologists, NY, Special Publ. No. 6, pp. 145–154.

Mahajan, S., Panwar, P., 2005. Land use changes in Ashwani Khad watershed using GIS Techniques. J. Indian Soc. Remote Sens. 33, 227–232.
Mohamed, I.N.L., Verstraeten, G., 2012. Analysing dune dynamics at the dune-field scale based on multi-temporal analysis of Landsat-TM images. Remote Sens. Environ. 119, 105–117.
Mohamed, E.S., Saleh, A.M., Belal, A.A., 2014. Sustainability indicators for agricultural land use based on GIS spatial modelling in North of Sinai – Egypt. Egypt. J. Remote Sens. Space Sci. 17, 1–15.
Mondal, M.S., Shrama, N., Kappas, M., Garg, P.K., 2013. Modeling of spatio-temporal dynamics of land use and land cover in a part of Brahmaputra river basin using Geoinformatic techniques. Geocarto Int. 28 (7), 632–656.
Nicoll, T.J., Hickin, E.J., 2010. Planform geometry and channel migration of confined meandering rivers on the Canadian prairies. Geomorphology 116, 37–47.
Ollero, A., 2010. Channel changes and floodplain management in meandering middle Ebro river, Spain. Geomorphology 117, 247–260.
Paolini, L., Grings, F., Sobrino, J.A., Munoz, J.C.J., Karszenbaum, H., 2006. Radiometric correction effects in Landsat multi-date/multi-sensor change detection studies. Int. J. Remote Sens. 27 (4), 685–704.
Qureshi, A.S., McCornick, P.G., Qadir, M., Aslam, Z., 2008. Managing salinity and waterlogging in the Indus Basin of Pakistan. Agric. Water Manage. 95, 1–10.
Rawat, J.S., Biswas, V., Kumar, M., 2013. Changes in land use/cover using geospatial techniques: a case study of Ramnagar town area, district Nainital, Uttarakhand, India. Egypt. J. Remote Sens. Space Sci. 16, 111–117.
Richards, J.A., Jia, X., 2006. Remote Sensing Digital Image Analysis – An Introduction, fourth ed. Springer-Verlag, Heidelberg, Germany.
Rogan, J., Chen, D.M., 2004. Remote sensing technology for mapping and monitoring land-cover and land-use change. Prog. Plan. 61, 301–325.
Rosenfield, G.H., Fitzpatrick, K., 1986. A coefficient of agreement as a measure of thematic classification accuracy. Photogramm. Eng. Remote Sens. 52, 223–227.
Roy, N., Sinha, R., 2007. Understanding confluence dynamics in the alluvial Ganga–Ramganga valley, India: an integrated approach using geomorphology and hydrology. Geomorphology 92, 182–197.
Sarma, J.N., Phukan, M.K., 2004. Origin and some geomorphological changes of Majuli Island of the Brahmaputra river in Assam, India. Geomorphology 60, 1–9.
Sarma, J.N., Borah, D., Goswami, U., 2007. Change of river channel and bank erosion of the Burhi Dihing river (Assam), assessed using remote sensing data and GIS. J. Indian. Soc. Remote. Sens. 35, 93–100.
Schulz, J.J., Cayuela, L., Echeverria, C., Salas, J., Benayas, J.M.R., 2010. Monitoring land cover change of dry land forest landscape of Central Chile. Appl. Geogr. 30, 436–447.
Schumm, S.A., 1963. Sinuosity of alluvial rivers on the Great Plains. Geol. Soc. Am. Bull. 74, 1089–1100.
Singh, A., 1989. Digital change detection techniques using remotely-sensed data. Int. J. Remote Sens. 10 (6), 989–1003.
Stolum, H.H., 1996. River meandering as self-organization process. Science 271 (5256), 1710–1713.
Sun, Z., Ma, R., Wand, Y., 2009. Using Landsat data to determine land use changes in Datong basin, China. Environ. Geol. 57, 1825–1837.
Sylla, L., Xiong, D., Zhang, H.Y., Bangoura, S.T., 2012. A GIS technology and method to assess environmental problems from land use/cover changes: Conarkry, Coyah and Dubreka region case study. Egypt. J. Remote Sens. Space Sci. 15, 31–38.
Tandon, S.K., Sinha, R., 2007. Geology of large rivers. In: Gupta, A. (Ed.), Large Rivers: Geomorphology and Management. John Wiley & Sons, 7, p. 28.
Thakur, P.K., Laha, C., Aggarwal, S.P., 2012. River bank erosion hazard study of river Ganga, upstream of Farakka barrage using remote sensing and GIS. Nat. Hazards 61, 967–987.
Tockner, K., Bunn, S.E., Gordon, C., Naiman, R.J., Quinn, G.P., Stanford, J.A., 2008. Flood plains: critically threatened ecosystems. In: Polunin, N. (Ed.), Aquatic Ecosystems: Trends and Global Prospect. Cambridge University Press, Cambridge, pp. 45–64.
Winterbottom, S.J., 2000. Medium and short-term channel planform changes on the Rivers Tay and Tummel, Scotland. Geomorphology 34, 195–208.
Yang, X., Lo, C.P., 2000. Relative radiometric normalization performance for change detection from multi-date satellite images. Photogramm. Eng. Remote Sens. 66 (8), 967–980.
Yao, Z., Ta, W., Jia, X., Xiao, J., 2011. Bank erosion and accretion along the Ningxia-Inner Mongoloia reaches of the yellow river from 1958 to 2008. Geomorphology 127, 99–106.
Yuan, F., Sawaya, K.E., Loeffelholz, B.C., Bauer, M.E., 2005. Land cover classification and change analysis of the Twin Cities (Minnesota). Remote Sens. Environ. 98, 317–328.